

Measurement of CP violation in $B_s \rightarrow J/\psi\phi$ decay

MICHAL KREPS

*Physics Department, University of Warwick
Gibbet Hill Road, Coventry, CV4 7AL, United Kingdom
M.Kreps@warwick.ac.uk*

We briefly discuss measurements of CP violation in $B_s \rightarrow J/\psi\phi$ decay. Both the phenomenology of B_s mixing and the importance of the measurement to searches for new physics, as well as technical details and issues with the analysis are included. While current results are consistent with the standard model, even large contributions from new physics cannot be excluded.

PACS numbers: 13.25.Hw, 11.30.Er, 14.40.Nd

Keywords: CP violation; $B_s \rightarrow J/\psi\phi$; B_s mixing.

I. INTRODUCTION

b -physics dates back to 1964 when the decay of the long lived kaon to two pions, and thus CP violation was observed [1]. It did not take very long until a proposal for the theoretical explanation of CP violation was made. In their famous work, Kobayashi and Maskawa showed that with 4 quarks there is no reasonable way to include CP violation [2]. Together with this, they also proposed several models to explain the observed CP violation in the kaon system, amongst which the six quark model became favored over time.

The explanation of CP violation in the six-quark model of Kobayashi and Maskawa builds on the idea of quark mixing introduced by Cabibbo. The quark mixing introduces a difference between eigenstates of the strong and weak interactions. CP violation requires a complex phase in order to provide a difference between a process and its charge conjugate. In the four-quark model, the quark mixing is described by a 2×2 unitarity matrix. With only four quarks, states can be always re-phased in order to keep the mixing matrix real and thus quark mixing cannot accommodate the observed CP violation. With the extension to six quarks, the mixing matrix becomes a 3×3 unitarity matrix, called the Cabibbo-Kobayashi-Maskawa matrix, V_{CKM} . In this case there is no possibility to rotate away all phases and one complex phase always remains in the matrix. This complex phase of V_{CKM} provides the CP violation in the standard model. This idea had two important implications. First, in addition to the three quarks known in the early 1970's and the predicted charm quark, it postulates the existence of two additional quarks, called bottom and top. Second, despite the tiny CP violation in the kaon system, the proposed mechanism implies large CP violation in the B^0 system. It took almost three decades, but both predictions were experimentally confirmed, first by the discovery of the bottom quark in 1977 [3] followed by that of the top quark in 1995 [4, 5] and finally by the measurement of large CP violation in the B^0 system in 2001 [6, 7]. The observation of large CP violation in B^0 decays confirmed the Kobayashi-Maskawa mechanism as the way to generate the CP violation in the standard model, this resulting

in the 2008 Nobel prize for Kobayashi and Maskawa.

After confirmation of the standard model, the focus shifted to the search for new physics. One of the most promising processes is B_s^0 mixing, governed by the CKM matrix element V_{ts} . Indirect information suggests V_{ts} to be almost real, which translates to the fact that the CP violation due to the B_s^0 mixing is expected to be tiny in the standard model. Amongst possible ways of accessing new physics in the B_s mixing, the measurement of CP violation in $B_s \rightarrow J/\psi\phi$ decay is considered as a golden way. In this paper we review the current status of the existing measurements in the $B_s \rightarrow J/\psi\phi$ decay, as well as the issues connected to the measurement itself. We will omit here many details in favour of providing a comparison of measurements from different experiments and discussing features which are not always emphasised. Details of separate measurements are available for CDF in Refs. [8–10], for $D\bar{0}$ in Refs. [11, 12] and for LHCb in Ref. [13].

This paper is organized as follows: In section II, we briefly discuss the phenomenology of B_s^0 oscillations. An overview of the basic components of the analysis is given in section III. In sections IV and V, we discuss in more detail, two main components, namely the determination of whether B_s^0 was produced as B_s^0 or \bar{B}_s^0 and the maximum likelihood fit. Section VI deals with the statistical issues encountered in the measurements. The results are given in section VII and the paper concludes with future prospects in section VIII.

Note on particle naming. As this topic requires the distinction between the use of both particle and anti-particle and the relevant single-flavour cases, we adopt a notation in which B_s denotes both particle B_s^0 and anti-particle \bar{B}_s^0 , while the use of B_s^0 or \bar{B}_s^0 denotes a given flavour.

II. PHENOMENOLOGY OF THE B_s^0 SYSTEM

The time evolution of the B_s^0 system is described by the Schrödinger equation

$$i \frac{d}{dt} \begin{pmatrix} |B_s^0(t)\rangle \\ |\bar{B}_s^0(t)\rangle \end{pmatrix} = \left(\hat{M} - \frac{i}{2} \hat{\Gamma} \right) \begin{pmatrix} |B_s^0(t)\rangle \\ |\bar{B}_s^0(t)\rangle \end{pmatrix},$$

where the 2×2 matrices \hat{M} and $\hat{\Gamma}$ describe the masses and decay rates. Diagonalization leads to eigenstates with definite masses and lifetimes

$$\begin{aligned} |B_s^H\rangle &= p |B_s^0\rangle + q |\bar{B}_s^0\rangle, \\ |B_s^L\rangle &= p |B_s^0\rangle - q |\bar{B}_s^0\rangle, \end{aligned}$$

with p and q being complex numbers satisfying $|p|^2 + |q|^2 = 1$. The states $|B_s^H\rangle$ and $|B_s^L\rangle$ have distinct masses M_H and M_L and distinct decay widths Γ_H and Γ_L . The B_s^0 mixing Feynman diagrams responsible for the transition of B_s^0 to \bar{B}_s^0 and vice versa give rise to the off-diagonal elements M_{12} and Γ_{12} . The B_s mixing observables are defined to be the mass difference between $|B_s^H\rangle$ and $|B_s^L\rangle$ states

$$\Delta M = M_H - M_L = 2|M_{12}| \quad (1)$$

and the decay width difference

$$\Delta\Gamma = \Gamma_L - \Gamma_H = 2|\Gamma_{12}| \cos \phi_s, \quad (2)$$

where $\phi_s = \arg(-M_{12}/\Gamma_{12})$. The standard model predictions [14, 15] are $\Delta M = (17.3 \pm 2.6) \text{ ps}^{-1}$, $\phi_s = (0.22 \pm 0.06)^\circ$ and $\Delta\Gamma = (0.087 \pm 0.021) \text{ ps}^{-1}$. Physics beyond the standard model can alter the picture by affecting both M_{12} and Γ_{12} . In practice most of the models of new physics consider only changes in $|M_{12}|$ and ϕ_s , and leave $|\Gamma_{12}|$ unaffected. The B_s^0 mixing frequency ΔM is measured most precisely by the CDF experiment [16] as $\Delta M = 17.77 \pm 0.10 \pm 0.07 \text{ ps}^{-1}$, and preliminary with similar precision also by LHCb [17] as $\Delta M = 17.63 \pm 0.11 \pm 0.04 \text{ ps}^{-1}$. Since ΔM is precisely known and consistent with the standard model expectation, new contributions to $|M_{12}|$ are strongly constrained. At the same time, Γ_{12} is dominated by the tree level $b \rightarrow c\bar{c}s$ transition and therefore it is non-trivial to construct a model which would affect $|\Gamma_{12}|$ significantly while at the same time avoiding constraints from existing measurements. The phase ϕ_s was experimentally unconstrained until recently, which made it the prime candidate for searches for new physics.

The B_s mixing phase ϕ_s can be accessed experimentally by measurements of the CP asymmetry in flavour-specific decays or by CP violation due to an interference between decays with and without mixing. The flavour-specific CP asymmetry is defined as

$$a_{fs}^s = \frac{|\Gamma_{12}|}{|M_{12}|} \sin(\phi_s). \quad (3)$$

The challenge of the a_{fs} measurement is in the smallness of the effect. If we assume no new physics contribution to $|\Gamma_{12}|$, then the maximum effect would be typically at most 5×10^{-3} and would not reach values above 10^{-2} even in the most optimistic scenario.

In the second type of measurement, one exploits a final state which is common to both B_s^0 and \bar{B}_s^0 . In such a case an interference between the amplitude for a direct decay of B_s^0 to a given final state and the amplitude for B_s^0 oscillating to \bar{B}_s^0 which then decays to the final state gives rise to a time-dependent CP violation. The decay $B_s \rightarrow J/\psi\phi$ which we are going to discuss in this review belongs to this category. A complication arises from the fact that this type of CP violation does not measure directly the ϕ_s but rather the relative phase between ϕ_s and the phase of the decay. For the decay $B_s \rightarrow J/\psi\phi$ the standard model expectation [18, 19] for the CP -violating phase is

$$\beta_s^{\text{SM}} = \arg\left(\frac{-V_{ts}V_{tb}^*}{V_{cs}V_{cb}^*}\right) \approx 0.02. \quad (4)$$

As mentioned before, the current focus is on the search for new physics. If new physics contributes to the B_s mixing process, it can modify the phase between M_{12} and Γ_{12} to $\phi_s = \phi_s^{\text{SM}} + \phi_s^{\text{NP}}$ where ϕ_s^{NP} is a new physics contribution. This new phase will then also be reflected in the measurement of $B_s \rightarrow J/\psi\phi$ decay where the observable phase can be expressed as

$$\phi_s^{J/\psi\phi} = -2\beta_s^{\text{SM}} + \phi_s^{\text{NP}}. \quad (5)$$

Here we have neglected possible higher order corrections to the decay both in the standard model as well as in new physics models. With the current generation of measurements the sensitivity is not sufficient to reach standard model values, but it is possible to search for large new physics contributions. While precise predictions for new physics models are not easily available, large effects are possible even after taking into account all existing constraints on possible new physics models. It is also worth noting that in many models of new physics, there is a correlation between the CP violation in B_s mixing and other flavour physics observables which can help to distinguish different new physics scenarios. For examples of a new physics discussion see Refs. [20–27].

Finally one remark on the notation which differs between experiments. Different symbols are used to denote the CP violation in $B_s \rightarrow J/\psi\phi$ decay and it is not always made fully clear how they are defined. On the other hand, given the precision of the existing measurements, the standard model contributions to the various phases can be neglected and we can interpret results as constraints on new physics contributions to the B_s mixing phase ϕ_s . In the following we will use the symbol $\phi_s^{J/\psi\phi}$ to denote the phase measured by experiment in $B_s \rightarrow J/\psi\phi$ decay. This relates to β_s used by CDF as $\phi_s^{J/\psi\phi} = -2\beta_s$ and is the same as the ϕ_s used by LHCb. In their latest documents, D0 uses the symbol $\phi_s^{J/\psi\phi}$.

III. MEASUREMENT OVERVIEW

The measurement of CP violation in $B_s \rightarrow J/\psi\phi$ decays is based on a time-dependent analysis. As the $J/\psi\phi$ final state is common to both B_s^0 and \bar{B}_s^0 , direct decays of the B_s^0 to $J/\psi\phi$ are possible, as well as the decay where the B_s^0 first oscillates to \bar{B}_s^0 and then decays. The two paths to the final state interfere and give rise to the CP violation. The main principle is to extract the time-dependent asymmetry

$$A(t) = \frac{N(B_s^0, t) - N(\bar{B}_s^0, t)}{N(B_s^0, t) + N(\bar{B}_s^0, t)}, \quad (6)$$

where $N(B_s^0, t)$ ($N(\bar{B}_s^0, t)$) is the number of $B_s \rightarrow J/\psi\phi$ decays at a given time t where B_s^0 (\bar{B}_s^0) was originally produced. Using this we can identify the main components of the analysis, which are the reconstruction and selection of the candidates, the measurement of the decay time for each candidate, and finding out whether a given candidate was produced as B_s^0 or \bar{B}_s^0 . While the concept is rather simple, the fact that both J/ψ and ϕ are spin-1 particles means that the final state is a mixture of CP -eigenstates. This adds to the complexity of the task as one needs to separate also CP -odd and CP -even components through an angular analysis. Therefore in the final step, rather than forming an asymmetry, a maximum likelihood fit is typically used to extract information on the CP violation. The first two steps are rather straightforward and we will discuss them shortly in this section; the others are those which require non-trivial work and therefore we discuss them in dedicated sections.

In all three experiments the $B_s \rightarrow J/\psi\phi$ decays are reconstructed using the J/ψ decays to two oppositely charged muons and the ϕ decays to oppositely charged kaons. The selection uses similar inputs in all three experiments. Events are typically selected by placing requirements on the momenta of reconstructed B_s candidates and their daughters, the quality of tracks, and the quality of kinematic fits where all four tracks are constrained to originate from a common vertex. LHCb, and to some extent also CDF, have particle identification capabilities, which are used to separate kaons from more abundant pions. While the LHCb and D0 experiments use sequential rectangular requirements, the CDF selection employs a neural network to distinguish signal events from a combinatorial background. An important aspect of the selection at CDF is that the requirement on the resulting neural network output is chosen to minimize the expected uncertainties on the measured CP violation. This is achieved by performing the analysis on simulated experiments, where each simulated experiment uses the number of signal and background events corresponding to the given requirement on the neural network output. An example of the outcome of simulation for the standard model CP violation is shown in Fig. 1. The simulations which included different size of the CP violation provide

the same picture. It is interesting to note that the resulting selection accepts more background than the procedure used in early CDF analysis. The selected sample comprises of 6504 ± 85 $B_s \rightarrow J/\psi\phi$ signal events at CDF, 3435 ± 84 signal events at D0 and 757 ± 28 $B_s \rightarrow J/\psi\phi$ decays at LHCb. The invariant mass distributions from all three experiments are shown in Figs. 1–3. It should be noted that LHCb selects only candidates with proper decay time larger than 0.3 ps while the Tevatron experiments accept all events independent of their decay time.

The decay time for each candidate is extracted from the displacement of the B_s decay vertex away from the primary vertex, which is reconstructed for each event separately. The uncertainty on the decay time can be estimated separately for each candidate and this can be exploited in the analysis. The typical resolution at the Tevatron experiments is about 80–100 fs while thanks to the higher boost the resolution at LHCb is of the order of 50 fs. The factor of 2 in the proper decay time resolution between Tevatron and LHCb gives a significant advantage to the LHCb experiment in resolving the fast B_s oscillations.

IV. FLAVOUR TAGGING

As mentioned before, the important part of the analysis is to determine whether a given candidate was produced as a B_s^0 or \bar{B}_s^0 . This task is performed by algorithms called flavour tagging and is one of the most challenging parts of the analysis.

At hadronic machines, most of the b quarks are produced in pairs of opposite flavour (charge). After hadronization, in the events interesting for the measurement, they end up in two independent b -hadrons. Given that many other particles are produced together with the b -hadrons, one can treat the two b -hadrons in the event as independent when considering their time evolution. This independence splits possibilities to tag flavour into two basic classes. The first one, called same side tagging, exploits the fragmentation process by which the B_s meson is created out of the b quark. The second class, called opposite side tagging, uses properties of the decay of the b -hadron which contains the other b quark. To fully characterize the performance of a flavour tagging algorithm, two quantities are needed. The first one is the efficiency, ϵ , which gives the fraction of the candidates for which a flavour tagging decision is made. The second one, called dilution, D , provides the information about the chance that the decision made is correct. Formally it is defined as

$$D = \frac{N_R - N_W}{N_R + N_W} = 2P_R - 1, \quad (7)$$

where N_R (N_W) is the number of correct (wrong) decisions and P_R is the probability of having the correct decision. Often the two performance quantities are combined

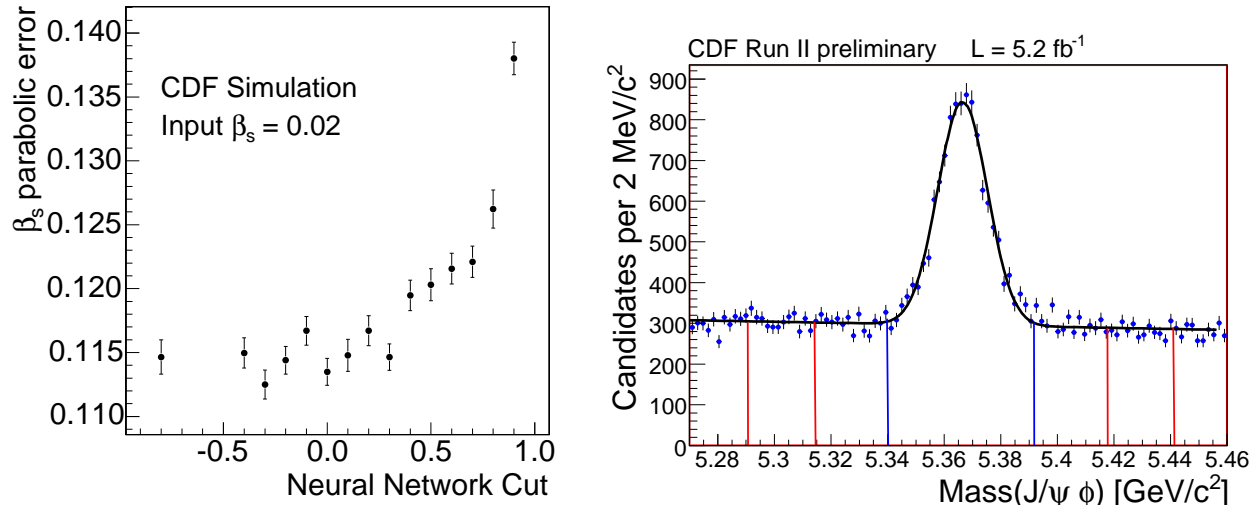


FIG. 1. Example of the dependence of the uncertainty on the CP violating phase as a function of the requirement on the neural network output at CDF (left). The invariant mass distribution of selected $B_s \rightarrow J/\psi \phi$ candidates at CDF (right).

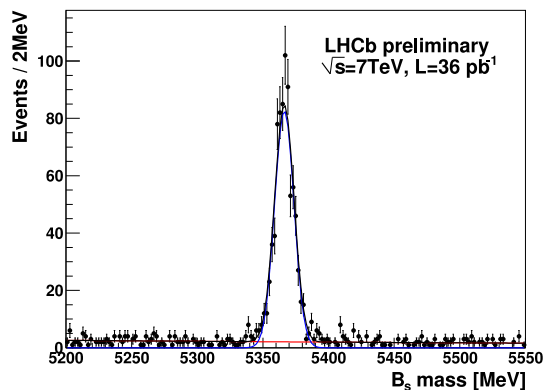


FIG. 2. The invariant mass distribution of the selected $B_s \rightarrow J/\psi \phi$ candidates at LHCb.

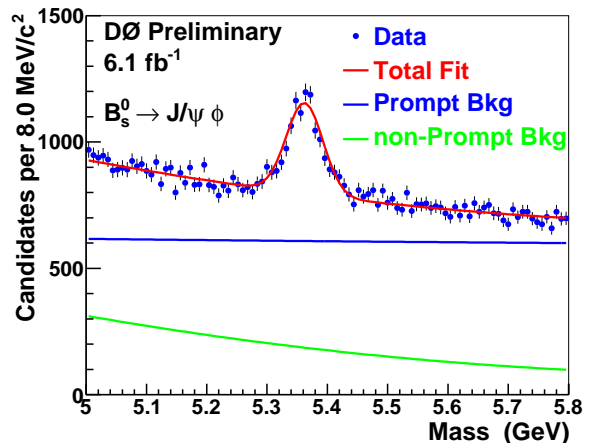


FIG. 3. The invariant mass distribution of the selected $B_s \rightarrow J/\psi \phi$ candidates at D0.

into a single value as ϵD^2 , which gives the effective statistics of the tagged sample. If we have N events with given flavour tagging performance, they will be equivalent to $N\epsilon D^2$ events with perfectly known production flavour. Typically the dilution is estimated on a candidate-by-candidate basis, and often used as additional information in the fits in order to increase the sensitivity to the oscillation behaviour of the B_s .

A. Flavour tagging algorithms

The physics idea behind the same side tagging is rather simple. In order to produce a B_s^0 , one needs to attach a strange quark to the bottom anti-quark in the hadronization process. The strange quark normally originates from

a pair of quark and anti-quark and thus the remaining strange anti-quark has to end up in another hadron. With significant chance this other hadron is a kaon. If it is a charged kaon and the experimentalist succeeds in picking-up the correct corresponding track, then the charge of the track determines also the flavour of the B_s^0 at the production time. While the general idea is rather simple, the details of the hadronization are far from being fully understood and therefore it is hard to develop such an algorithm. The selection of the tagging track can be done based on kinematical and/or particle identification information. From a point of view of kinematics, the track which carries the fragmentation partner will typically have small transverse momentum relative to the B_s and a large component of momentum in the direction of

the B_s . The particle identification is a significant help as most of the particles produced in pp or $p\bar{p}$ collisions are pions and therefore a track positively identified as a kaon and being close to the B_s has a large probability to be the right track.

The opposite side algorithms exploit the decay of the second b -hadron in the event. Once its flavour is determined, as the bottom quarks are produced in pairs of quark and anti-quark, the production flavour of the detected B_s can be taken as opposite.

The most common way of identifying the flavour of the other b -hadron is to exploit semileptonic decays. They have a rather large branching fraction and provide a unique and clear experimental signature. The charge of the lepton is directly correlated to the flavour of the b quark in the decaying hadron. All experiments use decays which contain either an electron or muon. As the leptons are dominantly produced by the decays of heavy flavour (b and c) quarks, there is a large chance that the identified lepton originates in the b -hadron decay.

The second piece of information which can be used for opposite-side tagging is based on the $b \rightarrow c \rightarrow s$ decay chain of the b quark with the strange quark ending up in kaon. If charged, it contains information about the flavour of the decaying b -hadron. Experimentally one is looking for a charged kaon, which does not point to the primary vertex.

The other piece of information to use is more inclusive and utilizes a jet charge by CDF experiment and a secondary vertex charge by D0 and LHCb. The jet charge is calculated for each jet as

$$Q_{\text{jet}} = \sum q_i p_T^i w_{NN}^i / \sum p_T^i w_{NN}^i, \quad (8)$$

where sums run over all tracks associated with the jet and q_i is the charge of the i -th track, p_T^i is the transverse momentum of the given track, and w_{NN}^i is the probability that the track originates from the b -hadron decay [28]. The calculated jet charge is then used to decide on the production flavour of the B_s meson. Three classes of jets are distinguished at CDF. The first class contains events with a secondary vertex within the jet. The second class is defined to contain events without a secondary vertex, but at least one track with a significant probability to come from b -hadron decay and the third class contains all events failing the criteria for the first two classes. The reason for the distinction is that different classes have different performance and distinguishing them helps to optimize the overall performance. The secondary vertex charge uses a similar strategy, but instead of using the full jet, it exploits tracks assigned to the secondary vertex. The charge is calculated as

$$Q_{SV} = \frac{\sum q_i w_i}{\sum w_i}, \quad (9)$$

where q_i is the charge of the track and w_i is the weight. There are several options for weights which are in principle equivalent. The D0 experiment uses as w_i , the longitudinal momentum of the track along the direction of

total momentum of the tracks assigned to the secondary vertex [29]. LHCb on the other hand uses as weight the transverse momentum of the track to the power of 0.4 [30].

In each of the three experiments the different algorithms are executed separately and their outputs are then combined together. Typically in the combinations, opposite side algorithms are combined to a single decision and then the same side algorithm, if used, is handled as uncorrelated to the opposite side decision. For combination of opposite side algorithms, CDF uses a neural network while D0 and LHCb use a likelihood method.

B. Calibration

All three experiments make an effort to calibrate the mistag probabilities directly on the data. It is useful to treat the opposite- and the same-side tagging separately. As the opposite side tagging is independent of the reconstructed b -hadron, it is possible to use the more abundant B^\pm and B^0 mesons for the calibration. On the other hand, same-side tagging depends on the b -meson under study and therefore has to be calibrated using the B_s mesons for the application discussed here.

1. Opposite side tagging

The easiest way of calibrating the opposite side tagging algorithms is to use fully reconstructed B^\pm decays. In the context of the measurement of the CP violation in $B_s \rightarrow J/\psi\phi$ decays, the most useful decay is $B^\pm \rightarrow J/\psi K^\pm$. The advantage of the B^\pm is given by the fact that its reconstruction efficiency is rather high due to the lower number of tracks needed in the reconstruction and more importantly that it does not oscillate. Therefore the charge obtained from the decay products unambiguously identifies the flavour at the production time. As the production flavour is known for each candidate, one can easily measure the probability P_R of having a correct decision and compare this with the probability estimated by the algorithm. The high abundance of the reconstructed B^\pm signal also allows the measurement of the flavour tagging asymmetry by splitting the sample into B^+ and B^- . As an example, Fig. 4 shows the invariant mass distribution of reconstructed B^\pm signal at CDF and the dependence of the measured dilution on the estimated dilution. In this case, the ideal behaviour is a linear dependence with a slope of unity. The slope itself is later used in the fit for the CP violation in $B_s \rightarrow J/\psi\phi$ to correct the estimated dilutions of the opposite-side taggers.

The second option for the calibration of the opposite-side tagging is to use B^0 decays and measure the oscillation pattern. It consists of measurement of the asymme-

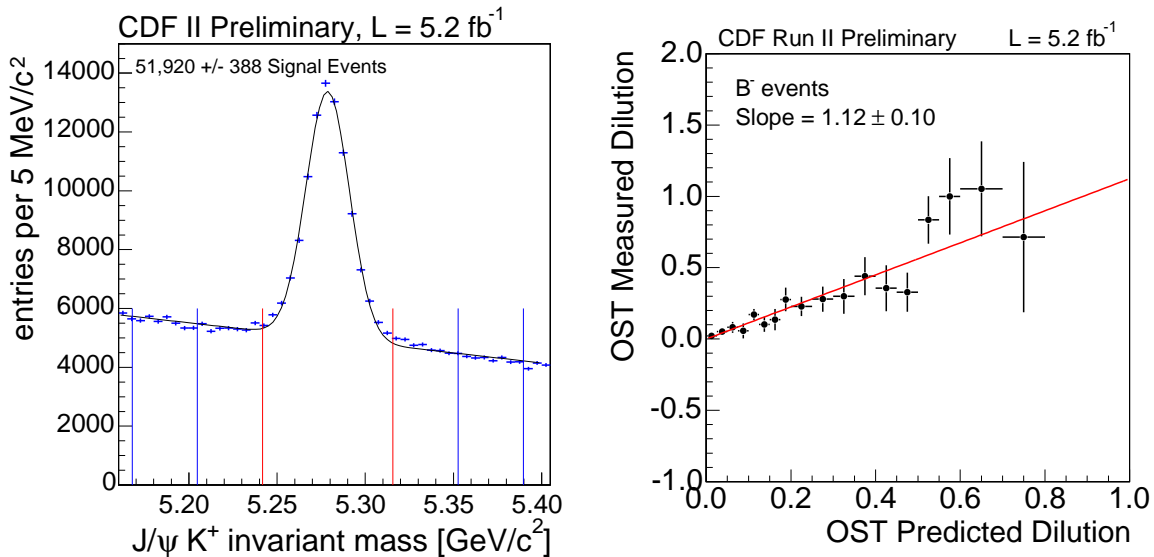


FIG. 4. Example of the opposite side flavour tagging calibration using $B^\pm \rightarrow J/\psi K^\pm$ decays at CDF. On the left we show the $J/\psi K^\pm$ invariant mass distribution showing clear B^\pm signal. On the right we show the measured dilution as a function of the estimated dilution for the B^- only.

try

$$A_{\text{mixing}}(t) = \frac{N_{\text{mix}}(t) - N_{\text{unmix}}(t)}{N_{\text{mix}}(t) + N_{\text{unmix}}(t)} \quad (10)$$

where N_{mix} (N_{unmix}) is the number of B^0 candidates with the same (opposite) flavour at the production and decay time. The amplitude of the asymmetry directly encodes the performance of the flavour tagging algorithm. While the achievable precision cannot compete with the B^\pm decays, it provides a demonstration that particle oscillations can be resolved and thus builds up the overall confidence in the analysis. While each of the three experiments performed the B^0 mixing measurement at some point on the way to current work on CP violation in B_s^0 , it is not widely used in the latest results due to its statistical limitations.

2. Same side tagging

A more difficult part is to calibrate the same side flavour tagging as it can be done only by using the B_s itself. The principle is the same as using B^0 to calibrate the opposite side tagging. Measuring the B_s oscillations using flavour-specific B_s decays, the asymmetry amplitude provides direct information on the flavour tagging power. The difficulty is in the lower B_s yield and the very fast oscillations, which make it hard to obtain a significant mixing signal. In addition, care has to be taken to properly describe the decay time resolution as its mis-modelling also affects the mixing asymmetry amplitude. On the other hand, one could argue that even if there is some decay time resolution mis-modeling, it is likely

to be the same as in the case of decay $B_s \rightarrow J/\psi \phi$ and therefore does not pose a real issue for the analysis.

To calibrate the same-side tagging, CDF uses the decays $B_s \rightarrow D_s^\mp \pi^\pm$ and $B_s \rightarrow D_s^\mp \pi^\pm \pi^+ \pi^-$. The D_s^- is reconstructed in decays to $\phi \pi^-$, $K^* K^-$ or $\pi^+ \pi^- \pi^-$, where for the decay $B_s \rightarrow D_s^\mp \pi^\pm \pi^+ \pi^-$, only the $D_s^- \rightarrow \phi \pi^\pm$ is used. Altogether about 12900 signal events are reconstructed. The same-side flavour tagging algorithm estimates for each candidate dilution, which is taken into account in the B_s oscillation fit. From the measured amplitude of the B_s mixing, CDF derives a single scaling factor for the estimated dilution of $A = 0.94 \pm 0.15(\text{stat}) \pm 0.13(\text{syst})$ [31]. In this approach, one cannot correct the shape of the dilution distribution, but only adjust the overall average scale of it.

The LHCb experiment plans to use the B_s mixing to calibrate the same side tagging. The first study using data collected in 2010 allowed the measurement of the B_s mixing frequency using the opposite-side flavour tagging [32]. While the measurement of the B_s^0 mixing was possible, the same side flavour tagging performance is not sufficient to obtain a significant signal with the same-side flavour tagging only. As a consequence the first measurement of the CP violation in $B_s \rightarrow J/\psi \phi$ from the LHCb experiment does not use the same-side flavour tagging.

The situation at D0 is different as there is no effective way to trigger on the hadronic decays. Therefore it is impossible to obtain sufficient statistics in the fully reconstructed flavour-specific decays. There is the possibility of reconstructing a large sample of semileptonic decays but due to the missing neutrino, the time resolution is significantly worse, which makes it difficult to obtain a significant B_s mixing signal. All this makes calibration of the same-side tagging at D0 very difficult and

the D0 experiment did not attempt to perform it up to now. It should be noted that while D0 used the same-side tagging in previous rounds of the analysis, the latest analysis does not use same-side flavour tagging.

C. Performance

The performance of the flavour tagging at the CDF experiment is $\epsilon D^2 \approx 1.2\%$ for the opposite-side algorithm and $\epsilon D^2 \approx 3.2\%$ for the same-side algorithm. As there is an overlap between the two taggers, it is not straightforward to combine the two numbers into the single performance number. The D0 experiment achieves for its opposite-side flavour tagging $\epsilon D^2 \approx 2.5\%$. Finally the opposite-side flavour tagging performance at the LHCb experiment is $\epsilon D^2 \approx 2.2\%$.

It is interesting to compare the CDF and D0 performances as the two detectors cover basically the same phase space region and work in the same environment. The factor two in the performance of the opposite side flavour tagging comes almost entirely from the better muon system, which has larger coverage at D0 compared to CDF, but also lower misidentification rate. On the other hand, CDF benefits from limited particle identification, which significantly boosts the performance of the same-side flavour tagging. The main drawback of the same-side flavour tagging is in calibration, which requires significant effort for quite limited precision.

The comparison between the Tevatron and LHCb experiments is more difficult as they cover different phase space regions. Despite that we can still safely say that LHCb strongly benefits from the excellent particle identification, which boosts their opposite-side flavour tagging by identification of kaons coming from the $b \rightarrow c \rightarrow s$ decay chain. Also, thanks to the forward geometry and design specific for flavour physics, the identification of electrons should be easier compared to the multi-purpose detectors at Tevatron. At the same time the same-side flavour tagging at LHCb is expected to perform worse than at CDF as the track density in the forward region is larger and thus it is more difficult to pick up the correct track. It should be also noted that in 2010, the LHCb experiment was taking data with the number of interactions per bunch crossing well above the design value, which means again a more difficult environment for the flavour tagging.

V. FIT DESCRIPTION

It is time to get to the heart of the analysis, which is a maximum likelihood fit. We are going to skip most of the details of the background description and refer the reader to the original work of the experiments. In short, the background is described using a phenomenological description derived mostly using data events in the B_s mass sidebands. The important part we want to discuss

in detail is the description of the B_s decays in the fit. It is rather instructive to read through the details in Refs. [33, 34]. The CDF analysis is based fully on the description in Ref. [33]. As we will discuss in the following, the LHCb and D0 analyses do not implement all the subtleties of the decay.

As we have already discussed, for each candidate which the experiments reconstruct, the flavour tagging determines whether the candidate was produced as a B_s^0 or \bar{B}_s^0 . In the following, this is encoded in the variable ξ , which takes values 1 for the B_s^0 , -1 for the \bar{B}_s^0 , and 0 if the flavour tagging is unable to make a decision. The signal probability function is given by the weighted average of the probability density functions for B_s^0 and \bar{B}_s^0 which takes the form

$$P_s(t, \vec{\rho}, \xi | D, \sigma_t) = \frac{1 + \xi D}{2} P(t, \vec{\rho} | \sigma_t) \epsilon(\vec{\rho}) + \frac{1 - \xi D}{2} \bar{P}(t, \vec{\rho} | \sigma_t) \epsilon(\vec{\rho}), \quad (11)$$

where P and \bar{P} are the probability density functions for B_s^0 and \bar{B}_s^0 . The quantities t and σ_t are the decay time and its uncertainty for a given candidate, $\vec{\rho}$ contains the measured decay angles in the transversity basis [35] and D is the dilution predicted for the given candidate. Finally $\epsilon(\vec{\rho})$ parametrizes the angular efficiency. It should be noted that each of the experiments has some minimum requirements on the momentum in order to be able to reconstruct a track and this requirement reflects in non-uniform angular efficiencies. This minimal requirement is a consequence of the geometry of the detector and is in principle very hard to avoid.

The decay time and angular distribution of the decay $B_s \rightarrow J/\psi \phi$ is given in Refs. [35] as

$$\begin{aligned} \frac{d^4 P(t, \vec{\rho})}{dt d\vec{\rho}} &\propto |A_0|^2 \mathcal{T}_+ f_1(\vec{\rho}) + |A_{\parallel}|^2 \mathcal{T}_+ f_2(\vec{\rho}) \\ &+ |A_{\perp}|^2 \mathcal{T}_- f_3(\vec{\rho}) + |A_{\parallel}| |A_{\perp}| \mathcal{U}_+ f_4(\vec{\rho}) \\ &+ |A_0| |A_{\parallel}| \cos(\delta_{\parallel}) \mathcal{T}_+ f_5(\vec{\rho}) \\ &+ |A_0| |A_{\perp}| \mathcal{V}_+ f_6(\vec{\rho}), \end{aligned} \quad (12)$$

where $|A_0|$, $|A_{\parallel}|$ and $|A_{\perp}|$ are three polarization amplitudes and the functions $f_i(\vec{\rho})$ describe the angular distributions [35]. The first three terms describe amplitudes-squared while the other three terms describe interferences between the three amplitudes. The description of \bar{B}_s^0 is obtained by substituting \mathcal{U}_+ by \mathcal{U}_- and \mathcal{V}_+ by \mathcal{V}_- . The functions \mathcal{T}_{\pm} , \mathcal{U}_{\pm} and \mathcal{V}_{\pm} provide the time dependence

and take the form

$$\mathcal{T}_{\pm} = e^{-\Gamma t} \times \left[\cosh(\Delta\Gamma t/2) \mp \cos(\phi_s^{J/\psi\phi}) \sinh(\Delta\Gamma t/2) \right. \\ \left. \pm \eta \sin(\phi_s^{J/\psi\phi}) \sin(\Delta m_s t) \right], \quad (13)$$

$$\mathcal{U}_{\pm} = \pm e^{-\Gamma t} \times \left[\sin(\delta_{\perp} - \delta_{\parallel}) \cos(\Delta m_s t) \right. \\ - \cos(\delta_{\perp} - \delta_{\parallel}) \cos(\phi_s^{J/\psi\phi}) \sin(\Delta m_s t) \\ \left. \mp \cos(\delta_{\perp} - \delta_{\parallel}) \sin(\phi_s^{J/\psi\phi}) \sinh(\Delta\Gamma t/2) \right] \quad (14)$$

$$\mathcal{V}_{\pm} = \pm e^{-\Gamma t} \times \left[\sin(\delta_{\perp}) \cos(\Delta m_s t) \right. \\ - \cos(\delta_{\perp}) \cos(\phi_s^{J/\psi\phi}) \sin(\Delta m_s t) \\ \left. \mp \cos(\delta_{\perp}) \sin(\phi_s^{J/\psi\phi}) \sinh(\Delta\Gamma t/2) \right]. \quad (15)$$

In this, δ_{\parallel} and δ_{\perp} are strong phases between amplitudes and η is 1 for B_s^0 and -1 for \bar{B}_s^0 .

There are a few interesting points to note which are different in this case compared to the analogous analysis of the CP violation in $B^0 \rightarrow J/\psi K_s^0$. First if we consider the case without flavour tagging, which corresponds to the case of $\xi = 0$ for each event, the terms $\sin(\Delta m_s t)$ cancel out, but there are several other terms which are sensitive to $\phi_s^{J/\psi\phi}$. This comes from the fact that both J/ψ and ϕ are spin 1 particles and thus we deal with a mixture of CP -even and CP -odd final states, which interferes and the non-zero $\Delta\Gamma$. As a benefit from this complexity, the system provides an additional sensitivity to the CP violation from the interference terms, which is available even without flavour tagging. The second point to note is that even if we put the CP violation to zero, equivalent to $\sin(\phi_s^{J/\psi\phi}) = 0$, the interference between CP -even and CP -odd provides sensitivity to the B_s mixing frequency [33] which can be exploited by experiments like ATLAS and CMS to perform a measurement also without access to the hadronic B_s decays. Finally, in the case of no CP violation one is sensitive to the strong phase δ_{\perp} only with the flavour tagging, while without the flavour tagging, δ_{\perp} is inaccessible.

A delicate issue is the question of a possible s-wave contribution to the reconstructed B_s signal. While each experiment has rather tight selection on the invariant mass of the kaon pair around the world average ϕ mass, decays like nonresonant $B_s \rightarrow J/\psi K^+ K^-$ or $B_s \rightarrow J/\psi f_0(980)$ with $f_0(980) \rightarrow K^+ K^-$ can contribute as well. Original estimates of the branching fraction relative to $B_s \rightarrow J/\psi\phi$ decay

$$R_{f_0/\phi} = \frac{\mathcal{B}(B_s \rightarrow J/\psi f_0(980)) \mathcal{B}(f_0(980) \rightarrow \pi^+ \pi^-)}{\mathcal{B}(B_s \rightarrow J/\psi\phi) \mathcal{B}(\phi \rightarrow K^+ K^-)} \quad (16)$$

yielded values around 0.2 [36]. While this estimate did not include the effect of the selection on the kaon pair invariant mass, it was argued that neglecting the s-wave contribution can bias the result for the CP violation [37]. Recent observation of the decay $B_s \rightarrow J/\psi f_0(980)$ and measurement of $R_{f_0/\phi}$ to be about 0.25 [38–41] further

support the necessity to take the s-wave contribution into account in some way. With a typical selection on the invariant mass of kaon pairs this would translate to about a 1.5% contribution from the $B_s \rightarrow J/\psi f_0(980)$ decay in the selected sample with rather large uncertainties due to badly known $f_0(980)$ branching fractions. At this stage the most complete treatment is done by the CDF experiment and uses the formalism from Ref. [33]. The analysis incorporates an additional amplitude yielding four more angular terms, one for the s-wave amplitude squared and three for the interference between the original amplitudes of the $B_s \rightarrow J/\psi\phi$ decay and the s-wave amplitude. The implementation treats the invariant mass of the kaon pair as an unobserved variable. While the s-wave complicates an already complex analysis further, it might provide an additional benefit in helping to resolve ambiguities in the value of the CP -violating phase. In contrast to the CDF treatment, neither D0 nor LHCb implements at this stage the s-wave contribution into the fit. As the presence of the significant s-wave contribution would introduce some asymmetry in the distribution of the kaon angle, experimentally it is possible to check for its presence. This was for the first time seen in the $B^0 \rightarrow J/\psi K^*$ decays at the Babar experiment [42]. The D0 experiment performs such a check by inspecting the forward-backward asymmetry in the kaon angle distribution in five different intervals of the kaon pair invariant mass (see Fig. 5). From

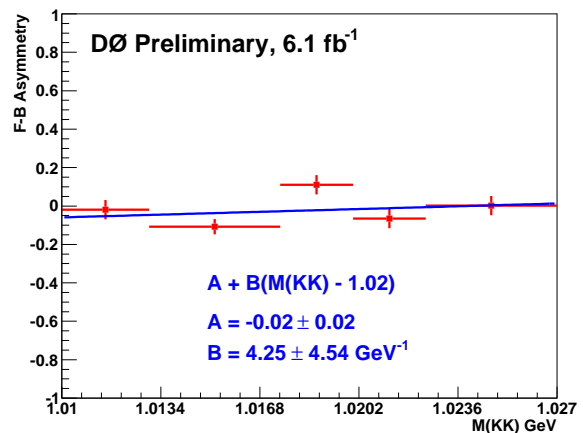


FIG. 5. The forward-backward asymmetry of the positive kaon angular distribution across the invariant mass of the kaon pair. In the absence of the s-wave, one expects a flat dependence, while in the presence, the dependence becomes non-trivial.

this they conclude that no significant s-wave is present and neglect it in the rest of the analysis. On the other hand, LHCb neglects s-wave contribution in the fit, but evaluates the systematic uncertainty using information on the s-wave derived by the CDF experiment in their full fit. Thus while none of the experiments has evidence for non-zero s-wave contribution, the CDF and LHCb experiments include such a possibility to the uncertainties, while D0 remains more aggressive and does not assign

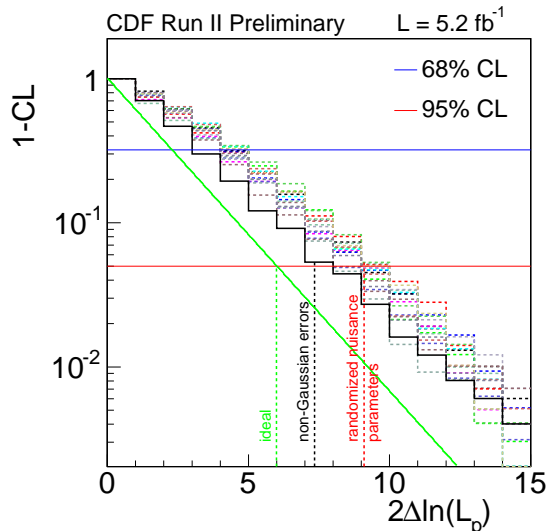


FIG. 6. The map between actual coverage and the likelihood ratio for the CDF measurement. The continuous line shows ideal Gaussian behaviour, the full histogram the default set of generated experiments and the dashed histograms show 16 alternative sets.

any uncertainties for the possible s-wave contribution.

VI. STATISTICAL ISSUES

While the interference between CP -odd and CP -even amplitudes helps in the determination of the CP violating phase $\phi_s^{J/\psi\phi}$, it also introduces some non-trivial statistical issues. As is apparent from Sec. V that the probability density function contains several periodic functions, resulting in some symmetries if we consider the $B_s \rightarrow J/\psi\phi$ decays without the s-wave contribution. Neglecting the s-wave contribution, the system is invariant under simultaneous transformation $\phi_s^{J/\psi\phi} \rightarrow \pi - \phi_s^{J/\psi\phi}$, $\Delta\Gamma \rightarrow -\Delta\Gamma$, $\delta_\perp \rightarrow \pi - \delta_\perp$, and $\delta_\parallel \rightarrow 2\pi - \delta_\parallel$. As a consequence there are two equivalent solutions which in the case of small statistics are not well separated. This fact itself makes minimization of the likelihood a difficult task. The issue of symmetries can appear not only for $\phi_s^{J/\psi\phi}$, but also for strong phases and, if their true values are close to the symmetry point, their extraction is again non-trivial.

As was discussed before, there is a possibility to extract information on the CP violation even without flavour tagging. In this case, the situation becomes even more difficult. The single symmetry of the flavour tagged case turns to two independent symmetries, which are $(\phi_s^{J/\psi\phi} \rightarrow -\phi_s^{J/\psi\phi}, \delta_\perp \rightarrow \delta_\perp + \pi)$ and $(\Delta\Gamma \rightarrow -\Delta\Gamma, \phi_s^{J/\psi\phi} \rightarrow \phi_s^{J/\psi\phi} - \pi)$. The consequence is the existence of four solutions compared to two in the flavour tagged case. An additional complication arises from the

fact that the strong phase δ_\perp appears always in a product with $\sin(\phi_s^{J/\psi\phi})$. As a result, in case of no CP violation there is no sensitivity to δ_\perp , but if the sensitivity to CP violation is small, the fit tends to bias the result as by increasing the CP violation, the fit gains δ_\perp as an additional parameter available to describe the statistical fluctuations. Moreover the bias is non-linear and decreases with increasing true CP violation.

It follows from the symmetries that there is a danger of non-Gaussian behaviour of the likelihood, which to some extent depends on the statistics and the true values of the parameters. If the true values are close to the symmetry points, more statistics are needed to clearly resolve those. Given the importance of the measurement for putting bounds on new physics, it is important to make sure that any non-Gaussian behaviour is properly taken into account. In order to achieve this, the experiments resort to a frequentist treatment based on the likelihood ratio ordering suggested by Feldman and Cousins [43]. To construct confidence level regions in the $\phi_s^{J/\psi\phi} - \Delta\Gamma$ plane, the procedure is to evaluate for each point, the ratio of likelihoods between the fit with $\phi_s^{J/\psi\phi}$ and $\Delta\Gamma$ fixed to specific values, and the fit where they are allowed to float. The likelihood ratio is then compared to the set of simulated experiments. For each point a p-value is obtained as a fraction of the number of simulated experiments which have a likelihood ratio larger than the one observed in the data. Connecting points with the same p-value yields the corresponding confidence-level region.

The difficulty in the procedure is that there are many parameters involved, for which we do not know the true values, but only estimates from experiments which could be from the analysis itself or some measurement external to the analysis. To deal with this, CDF generates one set of experiments using the values of all parameters except $\phi_s^{J/\psi\phi}$ and $\Delta\Gamma$ from the global minimum of the likelihood together with 16 alternative sets where all parameters are chosen randomly from a $\pm 5\sigma$ hypercube around the global minimum. An example of the map between the actual coverage and the likelihood ratio for the CDF experiment is shown in Fig. 6. While the procedure does not guarantee the exact coverage of the derived contours, it is assured that there is no undercoverage. The LHCb experiment employs a similar procedure, but from the available information it is not fully clear to what extent they vary the input parameters in the simulated experiments. The D0 experiment decides to take a different path and rather than going through a full frequentist treatment, they constrain the strong phases to the values measured in the $B^0 \rightarrow J/\psi K^*$ decay. This point is rather controversial with theoretical arguments supporting it presented in Ref. [44], but the argument is generally not fully accepted. From the experimental point of view, the constraint effectively removes some symmetries and better separates two minima. This results in a likelihood which is closer to the Gaussian shape, but still needs a small adjustment, which is performed in a similar way to

CDF and LHCb.

To finish the discussion on the statistical issues, a note on the importance of the flavour tagging and the time resolution is in order. As we discussed, there are two pieces of information about the CP violation in the analysis. The first one is in the interference between CP -even and CP -odd amplitudes and this one does not require the resolution of the B_s oscillations. Therefore the time resolution for this part is not critical. On the other hand, the importance is driven by the size of $\Delta\Gamma$. With larger $\Delta\Gamma$, the importance increases. As a consequence, there is some correlation between the uncertainty on $\phi_s^{J/\psi\phi}$ and the value of $\Delta\Gamma$ extracted by a given experiment. The second part of the sensitivity comes from resolving the B_s oscillations and here the flavour tagging performance and the time resolution are crucial. Here LHCb has the clear benefit of better time resolution compared to the Tevatron experiments. On the other hand, the flavour tagging performance is behind the CDF experiment at this stage and smears out part of the benefit from their better decay time resolution.

VII. RESULTS

Typically in each case two different fits are performed. One in which no CP violation is assumed and the values of physics parameters such as mean lifetime, decay width difference, and amplitudes are measured, and the second fit in which constraints on CP violation are derived. The main result of the analysis is given as bounds in the $\Delta\Gamma$ - $\phi_s^{J/\psi\phi}$ plane.

In Fig. 7 we show the confidence level contours in the $\Delta\Gamma$ - $\phi_s^{J/\psi\phi}$ plane from the CDF and D0 experiments and in Fig. 8, we show the contours derived by the LHCb experiment. The reader should be aware that CDF uses a different convention than D0 and LHCb with $-2\beta_s = \phi_s^{J/\psi\phi}$. As the standard model is a special case, each experiment derives consistency between the data and the standard model. The consistency is characterized by the p-value, which is 44% at CDF corresponding to about 0.8 standard deviations and LHCb finds a p-value of 22% which corresponds to about 1.2 standard deviations. Those tests provide an answer to the question of whether both $\Delta\Gamma$ and $\phi_s^{J/\psi\phi}$ are simultaneously consistent with the standard model. D0 does not evaluate an answer to this question, but from Fig. 7 we can see that the agreement is equivalent to little more than one standard deviation. It is worth noting that while CDF and LHCb allow for two solutions and therefore have bounds which are symmetric, D0, by constraining the strong phases, allows only for one solution. The fact that there are still two solutions in their result is an artefact of additional approximate symmetries of the problem. Some difference between those approximately symmetric solutions is seen, but the statistics are not sufficient to decide between them. Before moving on, we

come back to the point of deriving constraints without flavour tagging. In Fig. 9 we show constraints from the untagged analysis of the CDF experiments together with the result from Fig. 7. As one can see the size of the contours is not very different between the two analyses and the main help from the flavour tagging is in removing two out of the four solutions. The slight shift of the two results is due to the difference in the importance of each candidate for two analyses. The untagged analysis was performed by LHCb but no useful constraint could be derived with the current statistics [45]. D0 also performed a fit without flavour tagging and obtained a result consistent with the tagged fit.

What is more interesting for some people is simply the value of the CP -violating phase $\phi_s^{J/\psi\phi}$, rather than the allowed region in two-dimensional space. To obtain this, CDF and LHCb basically repeat the procedure used for the two-dimensional case where $\Delta\Gamma$ is also treated as an unimportant parameter and maximize likelihood over it. The procedure yields $\phi_s^{J/\psi\phi} \in [-3.1, -2.16] \cup [-1.04, -0.04]$ at 68% confidence level and $\phi_s^{J/\psi\phi} \in [-\pi, -1.78] \cup [-1.36, 0.26] \cup [2.88, \pi]$ at 95% confidence level at the CDF experiment. At LHCb the allowed regions are $\phi_s^{J/\psi\phi} \in [-2.7, -0.5]$ at 68% confidence level and $\phi_s^{J/\psi\phi} \in [-3.5, 0.2]$ at 95% confidence level. The D0 experiment does not provide a result in this way, but their values can be translated into approximate one-dimensional results as the correlation between $\Delta\Gamma$ and $\phi_s^{J/\psi\phi}$ is reasonably small, about -18% . The intervals they obtain are $\phi_s^{J/\psi\phi} \in [-1.12, -0.38]$ at 68% confidence level and $\phi_s^{J/\psi\phi} \in [-1.65, 0.24] \cup [1.14, 2.93]$ at 95% confidence level without taking into account any correction for non-Gaussian behaviour. Also in the case of one-dimensional tests, there is a reasonable agreement between the standard model and data.

As the CDF analysis implements also an s-wave contribution, it was possible to check also how large an effect it introduces. First, in Fig. 10 we show the likelihood profile for the amount of s-wave contribution and the invariant mass of the kaon pair, which is not used in the fit. From the full angular fit the obtained s-wave fraction is consistent with zero. From the likelihood profile one can set a Bayesian upper limit of about 7% at 95% credibility level for the s-wave fraction within the selected sample. One should note that this fraction is selection-dependent. As a cross-check one can also check whether the kaon pair invariant mass is consistent with the composition found in the full angular fit. We show the distribution together with the fit where the s-wave fraction is fixed to the best value from the angular fit in Fig. 10. As one can see, the model fits the data well and therefore adds additional confidence into the treatment adapted by the CDF experiment. Finally also a check for the effect of the s-wave can be made. In this CDF compared likelihood contours between fits with the s-wave allowed to float, and a fit with the s-wave fraction fixed to zero, and there is almost

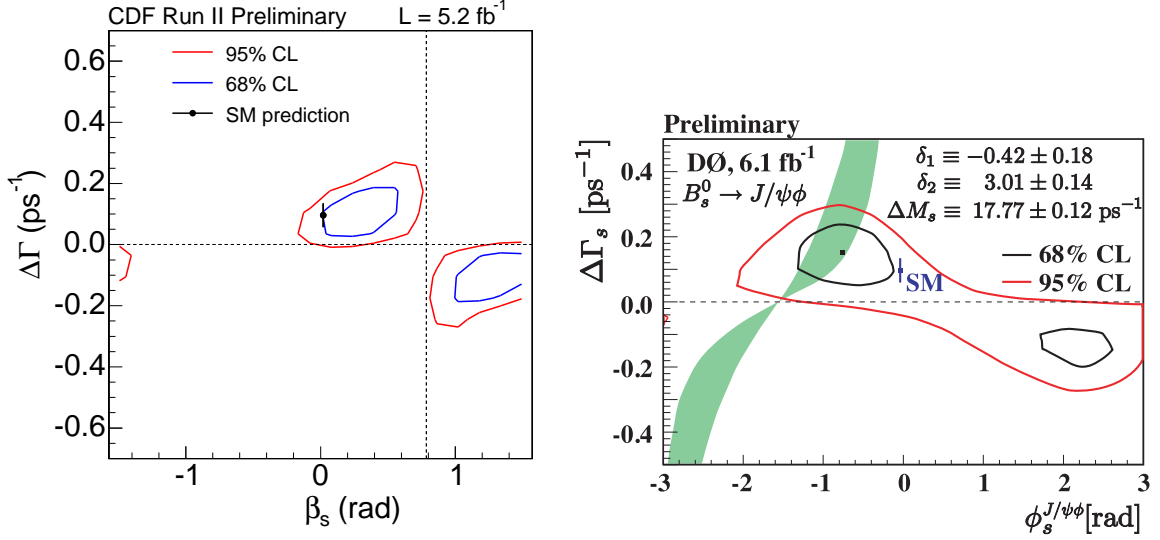


FIG. 7. The bounds in the $\Delta\Gamma$ - $\phi_s^{J/\psi\phi}$ plane obtained by the CDF (left) and D0 (right) experiments. Note that CDF is using the convention where $-2\beta_s = \phi_s^{J/\psi\phi}$.

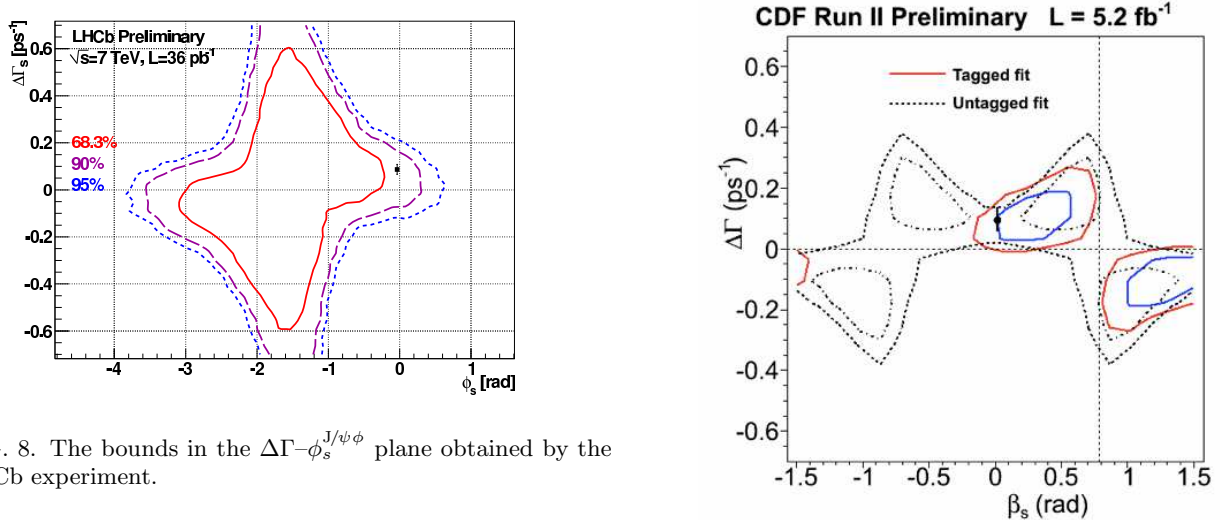


FIG. 8. The bounds in the $\Delta\Gamma$ - $\phi_s^{J/\psi\phi}$ plane obtained by the LHCb experiment.

no visible difference between them. For completeness we show results for the lifetime and $\Delta\Gamma$ in Fig. 11. They are typically obtained in a fit which assumes no CP violation and should therefore be treated in the context of the standard model. For results on the amplitudes we kindly refer the reader to the original work of the three experiments.

The important question is what the measurements tell us about the validity of the standard model and potential new physics contributions. In all three experiments, the evaluation of the consistency with the standard model is available and in all three cases there is no significant departure from the standard model. On the other hand, solutions obtained in all three experiments go in the same direction from the standard model which suggests that there might be some effect of new physics. While the

FIG. 9. The comparison of bounds in $\Delta\Gamma$ - β_s plane obtained by the flavour-tagged (full lines) and the flavour-untagged (dashed lines) analysis from the CDF experiment.

combination would be interesting, unfortunately with the information publicly available it is not possible to combine the results. Moreover with the current precision it is not possible to exclude any CP violation provided it lies in the half-plane in which all the results are. Therefore practically any constraints on new physics models from measurements presented here will be rather weak. This might not necessarily be the case when combined with measurements of other quantities, but such a discussion is beyond the scope of this review.

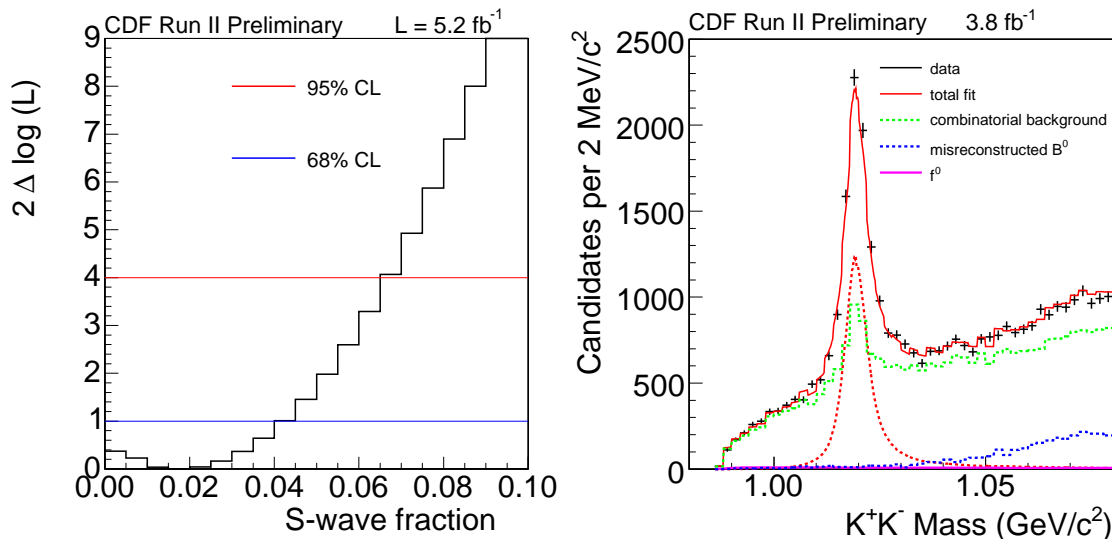


FIG. 10. The likelihood profile over the s-wave fraction from the full angular fit at CDF (left). The invariant mass of the kaon pair together with the fit from the CDF experiment (right). The fit itself includes the s-wave with fraction fixed from the full angular fit.

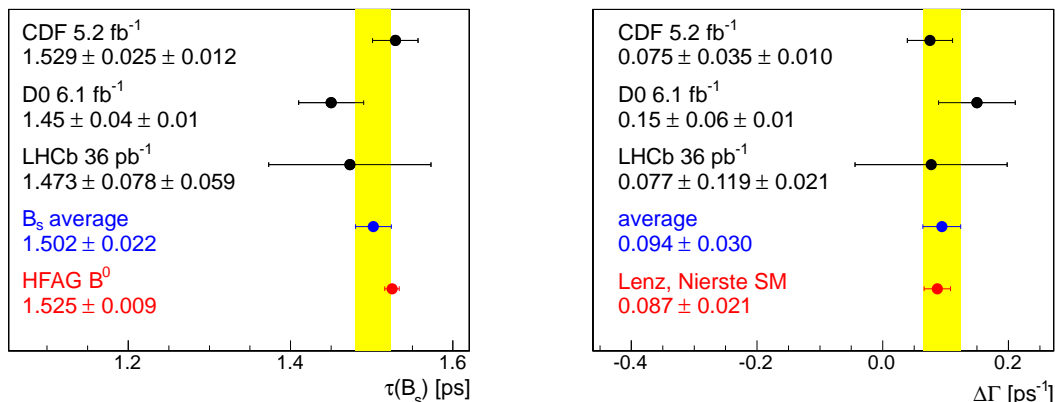


FIG. 11. The comparison of the measured mean lifetimes together with the B^0 lifetime which is predicted to be the same with high accuracy (left) and the decay width difference $\Delta\Gamma$ (right).

VIII. PROSPECTS

What to expect in the near future? There are good prospects to see new results within a couple of months. The Tevatron collider runs well and both CDF and D0 expect to collect about 10 fb^{-1} of data by the end of September 2011 when the Tevatron will terminate its operation. While some improvements would still be possible, we do not expect a large gain beyond the increased statistics. In the meantime, LHC performance is excellent with LHCb on track to collect about 1 fb^{-1} of data by the end of this year. Given that the first analysis was performed on only 37 pb^{-1} this gives good prospects for a large statistical improvement. Moreover as LHCb is an

experiment which started to take data only last year it is reasonable to expect some improvements which could help to constrain the CP violation in B_s mixing. Finally while the ATLAS and CMS experiments did not present results in this area, measurement of the CP violation in $B_s \rightarrow J/\psi\phi$ decay is in their plans with first results expected in the near future. To conclude, in the near future the precision might be sufficient to see significant signal of large CP violation in $B_s \rightarrow J/\psi\phi$ decay or constrain it to values close to the standard model. If it is constrained close to the standard model, then question of the suppressed standard model contributions will become important and could limit capability of bounding new physics until progress on the understanding suppressed standard model contribution is made [46–48].

-
- [1] J. H. Christenson, J. W. Cronin, V. L. Fitch, and R. Turlay, *Phys. Rev. Lett.* **13**, 138–140 (1964).
- [2] M. Kobayashi and T. Maskawa, *Prog. Theor. Phys.* **49**, 652–657 (1973).
- [3] S. W. Herb et al., *Phys. Rev. Lett.* **39**, 252–255 (1977).
- [4] S. Abachi et al. (D0 Collaboration), *Phys. Rev. Lett.* **74**, 2422–2426 (1995), arXiv:hep-ex/9411001.
- [5] F. Abe et al. (CDF Collaboration), *Phys. Rev. Lett.* **74**, 2626–2631 (1995), arXiv:hep-ex/9503002.
- [6] B. Aubert et al. (BABAR Collaboration), *Phys. Rev. Lett.* **86**, 2515–2522 (2001), arXiv:hep-ex/0102030.
- [7] K. Abe et al. (Belle Collaboration), *Phys. Rev. Lett.* **87**, 091802 (2001), arXiv:hep-ex/0107061.
- [8] T. Aaltonen et al. (CDF Collaboration), *Phys. Rev. Lett.* **100**, 161802 (2008), arXiv:0712.2397.
- [9] T. Aaltonen et al. (CDF Collaboration), CDF Public Note 9458, 2008 (unpublished).
- [10] T. Aaltonen et al. (CDF Collaboration), CDF Public Note 10206, 2010 (unpublished).
- [11] V. M. Abazov et al. (D0 Collaboration), *Phys. Rev. Lett.* **101**, 241801 (2008), arXiv:0802.2255.
- [12] V. M. Abazov et al. (D0 Collaboration), D0 Conference Note 6098–CONF, 2010 (unpublished).
- [13] R. Aaij et al. (LHCb Collaboration), LHCb Conference Note LHCb–PHIS–001, 2011 (unpublished).
- [14] A. Lenz and U. Nierste, *JHEP* **0706**, 072 (2007), arXiv:hep-ph/0612167.
- [15] A. Lenz and U. Nierste, in *Proceedings of CKM2010, the 6th International Workshop on the CKM Unitarity Triangle, University of Warwick, UK, 6-10 September 2010*, arXiv:1102.4274.
- [16] A. Abulencia et al. (CDF Collaboration), *Phys. Rev. Lett.* **97**, 242003 (2006), arXiv:hep-ex/0609040.
- [17] R. Aaij et al. (LHCb Collaboration), LHCb Conference Note LHCb–CONF–2011–005, 2011 (unpublished).
- [18] J. Charles et al., *Eur. Phys. J. C* **41**, 1–131 (2005), arXiv:hep-ph/0406184.
- [19] M. Bona et al., *JHEP* **0610**, 081 (2006), arXiv:hep-ph/0606167.
- [20] W. Hou, M. Nagashima, and A. Soddu, *Phys. Rev. D* **76**, 016004 (2007), arXiv:hep-ph/0610385.
- [21] A. J. Buras, M. Nagai, and P. Paradisi, *JHEP* **1105**, 005 (2011), arXiv:1011.4853.
- [22] A. Lenz, U. Nierste, J. Charles, S. Descotes-Genon, A. Jantsch, C. Kaufhold, H. Lacker, S. Monteil, V. Niess, and S. T’Jampens, *Phys. Rev. D* **83**, 036004 (2011), arXiv:1008.1593.
- [23] A. J. Buras, M. V. Carlucci, S. Gori, and G. Isidori, *JHEP* **1010**, 009 (2010), arXiv:1005.5310.
- [24] M. Bauer, S. Casagrande, U. Haisch, and M. Neubert, *JHEP* **1009**, 017 (2010), arXiv:0912.1625.
- [25] A. Soni, A. K. Alok, A. Giri, R. Mohanta, and S. Nandi, *Phys. Rev. D* **82**, 033009 (2010), arXiv:1002.0595.
- [26] C. Chiang, A. Datta, M. Duraisamy, D. London, M. Nagashima, and A. Szykman, *JHEP* **1004**, 031 (2010), arXiv:0910.2929.
- [27] C. Chen, *Phys. Lett. B* **683**, 160–164 (2010), arXiv:0911.3479.
- [28] C. Lecci, Ph.D. Thesis, Karlsruhe University, 2005.
- [29] V. M. Abazov et al. (D0 Collaboration), *Phys. Rev. D* **74**, 112002 (2006), arXiv:hep-ex/0609034.
- [30] M. Calvi, O. Leroy, M. Musy, LHCb Note LHCb–2007–058, 2007 (unpublished).
- [31] T. Aaltonen et al. (CDF Collaboration), CDF Public Note 10108, 2010 (unpublished).
- [32] R. Aaij et al. (LHCb Collaboration), LHCb Conference Note, LHCb–CONF–2011–005, 2011 (unpublished).
- [33] F. Azfar et al., *JHEP* **11**, 158 (2010), arXiv:1008.4283.
- [34] Y. Xie, P. Clarke, G. Cowan, and F. Muheim, *JHEP* **09**, 074 (2009), arXiv:0908.3627.
- [35] A. S. Dighe, I. Dunietz, H. J. Lipkin, and J. L. Rosner, *Phys. Lett. B* **369**, 144–150 (1996), arXiv:hep-ph/9511363.
- [36] S. Stone and L. Zhang, *Phys. Rev. D* **79**, 074024 (2009), arXiv:0812.2832.
- [37] S. Stone, PoS FPCP2010, 011 (2010), arXiv:1009.4939.
- [38] R. Aaij et al. (LHCb Collaboration), *Phys. Lett. B* **698**, 115–122 (2011), arXiv:1102.0206.
- [39] J. Li et al. (Belle Collaboration), *Phys. Rev. Lett.* **106**, 121802 (2011), arXiv:1102.2759.
- [40] T. Aaltonen et al. (CDF Collaboration), arXiv:1106.3682, 2011, submitted to *Phys. Rev. D*.
- [41] V. M. Abazov et al. (D0 Collaboration), D0 Conference Note 6152–CONF, 2011 (unpublished).
- [42] B. Aubert et al. (BABAR Collaboration), *Phys. Rev. D* **76**, 031102 (2007), arXiv:0704.0522.
- [43] G. J. Feldman and R. D. Cousins, *Phys. Rev. D* **57**, 3873–3889 (1998), arXiv:physics/9711021.
- [44] M. Gronau and J. L. Rosner, *Phys. Lett. B* **669**, 321–326 (2008), arXiv:0808.3761.
- [45] R. Aaij et al. (LHCb Collaboration), LHCb conference note LHCb–CONF–2011–002, 2011 (unpublished).
- [46] S. Faller, R. Fleischer, and T. Mannel, *Phys. Rev. D* **79**, 014005 (2009), arXiv:0810.4248.
- [47] M. Ciuchini, M. Pierini, and L. Silvestrini, *Phys. Rev. Lett.* **95**, 221804 (2005), arXiv:hep-ph/0507290.
- [48] M. Ciuchini, M. Pierini, and L. Silvestrini, in *Proceedings of CKM2010, the 6th International Workshop on the CKM Unitarity Triangle, University of Warwick, UK, 6-10 September 2010*, arXiv:1102.0392.